Available online at http://scik.org
J. Math. Comput. Sci. 2024, 14:13
https://doi.org/10.28919/jmcs/8794
ISSN: 1927-5307

MATHEMATICAL MODELING OF THE EFFECT OF IMMUNOSUPPRESSIVE THERAPY ON WITHIN-HOST EBOLA VIRUS DISEASE DYNAMICS

SELEMAN ISMAIL*

Department of Mathematics and Information and Communication Technology, Open University of Tanzania, P. O. Box 23409, Dar es Salaam, Tanzania

Abstract. Immunosuppressive therapy, a keystone of many treatments, can weaken the immune system, potentially worsening viral infections such as Ebolavirus disease (EVD). This study used mathematical modeling and simulations to explore the impact of immunosuppression on within-host EVD. The model integrates viral replication, the patient's immune response and the effect of immunosuppressive therapy. Simulations explored how varying degrees of immunosuppression influence the progression of EVD. Critically, the model predicted a direct correlation: increased immunosuppression triggered a noticeable rise in viral replication and a corresponding weakening of the immune response. This in silico approach provides valuable understandings of the complex interaction between EVD, the immune system and immunosuppressive therapy. The findings stress the potential risks associated with immunosuppression during EVD and emphasize the importance of considering these factors when making critical treatment decisions for EVD patients requiring such therapy.

Keywords: ebolavirus disease; immune response; immunosuppressive therapy; mathematical modeling; within-host EVD dynamics.

2020 AMS Subject Classification: 92D30.

*Corresponding author
E-mail address: selemanismail@yahoo.com
Received July 30, 2024

1. INTRODUCTION

Ebolavirus disease (EVD), caused by the Ebola virus (EBOV), is a terrifying hemorrhagic fever with a forbidding reputation for high mortality rates. The 2014-2016 West African Ebola virus epidemic tragically demonstrated the overwhelming potential of this pathogen, with over 28,600 confirmed, probable, and suspected cases and more than 11,300 deceases reported [41]. While major steps have been made in developing vaccines and treatments for EVD infection [15, 17, 35, 44], managing patients with weakened immune systems remains a critical challenge.

Organ transplantation, autoimmune diseases and various cancers generally necessitate immunosuppressive therapy. This treatment deliberately weakens the body's immune response, specifically cytotoxic T lymphocytes (CTLs) and antibody production, to stop organ rejection or autoimmune damage [1]. However, this vital therapy leaves patients weak to opportunistic infections, including those triggered by viruses like Ebolavirus. In EVD, the aggressive nature of the virus and the critical role of both CTLs and antibodies in controlling viral replication make the potential consequences of immunosuppression particularly concerning [14].

Understanding the intricate interaction between EBOV infection, the immune response and the effects of immunosuppressive therapy is essential for optimizing patient care during EVD outbreaks. Mathematical modeling emerges as a powerful tool for investigating these complex dynamics. By constructing models that represent the biological processes involved, researchers can gain valuable insights into how immunosuppression alters the progression of EVD infection [34].

Several recent studies have used mathematical modeling to explore viral dynamics and immune response, vaccine efficacy and treatment optimization of within-host EBOV infection [4, 5, 7, 8, 10, 11, 23, 28, 31, 32, 38, 39, 44]. A 2020 study by Chertow et al. [11] employed a mathematical model to investigate the interaction between viral kinetics, host immune response and potential treatment effects in EVD patients. Their model provided insights into the complex dynamics of viral load and immune cell activity during infection. A 2023 study by Li et al. [28] employed a modeling approach to assess the potential impact of different vaccination strategies on reducing viral burden and improving patient outcomes. A 2022 study by Wang et al. [44] investigated the potential application of Clustered Regularly Interspaced Short Palindromic Repeats (CRISPR) gene editing technology for EVD treatment using a mathematical framework. This research paves the way for exploring novel therapeutic strategies. Similarly, a 2021 study by Gao et al. [8] focused on modeling the immune response to EBOV vaccination. Their model

investigated the interaction between different immune cell populations and the development of protective immunity, paving the way for optimizing vaccine design.

Our current study builds upon this existing body of research by concentrating specifically on the impact of immunosuppressive therapy on EBOV infection dynamics within a patient. By using a mathematical model that includes viral replication, immune response elements, and the effects of immunosuppression, we aim to answer the following main questions: How does the degree of immunosuppression influence the rate of viral replication in an EVD patient? What impact does immunosuppression have on the effectiveness of the patient's immune response against EBOV? Can the model identify potential therapeutic strategies to alleviate the undesirable effects of immunosuppression during EVD treatment? By addressing these questions, this study seeks to contribute valuable knowledge to the management of EVD in immunocompromised patients. This knowledge can enlighten clinical decision-making regarding immunosuppressive therapy and guide the development of targeted interventions to improve patient outcomes during EVD outbreaks.

The existing body of research on EVD has principally focused on understanding the transmission dynamics and developing vaccines [9, 12]. While these efforts are crucial, a critical gap exists in our understanding of how immunosuppression influences EVD progression in individual patients [33]. This gap impedes the development of optimal treatment strategies for immunocompromised individuals who contract EVD. Our study aims to bridge this gap using mathematical modeling to explore the complex interaction between immunosuppression, viral replication and the immune response in the context of EVD.

2. MATERIALS AND METHODS

2.1 Model Development

This study employed a novel mathematical model built on a system of five ordinary differential equations (ODEs). These equations tracked the dynamic changes in key factors of EVD infection over time. The model specifically captured the rates of change for:

1. Susceptible target cell population (S): This variable represents the number of uninfected macrophages, dendritic cells and endothelial cells that are prone to Ebolavirus infection.
2. Infected cell population (I): This variable reflects the number of cells actively harboring the virus.
3. Ebolavirus (V): This variable denotes the number of virus particles present in the patient.

4. CTL population (T): This variable tracks the number of CTLs, immune cells crucial for eliminating infected cells.
5. Antibody population (B): This variable tracks the number of antibodies proteins vital for clearing the virus from the body.

Additionally, the model incorporated the impact of immunosuppressive therapy and how EVD infects macrophages and dendritic cells, since these processes significantly influence the development of both CTL and antibody responses.

2.2 Model Parameterization

To parameterize the model, we employed existing scientific literature on EVD infection, immune response dynamics and the effect of immunosuppressive therapy. A comprehensive list and descriptions of these parameters are provided in Table 1.

TABLE 1. Descriptions of parameters

Parameter	**Description**
η	Infection rate of susceptible cells.
γ_A	Natural death rate of susceptible and infected cells.
γ_B	Natural death rate of CTLs.
γ_C	Natural death rate of the virus.
γ_D	Natural death rate of antibodies.
μ_A	CTL-mediated infected cell elimination rate.
μ_B	Clearance rate of the viruses by antibodies.
μ_C	CTL proliferation rate.
μ_D	Antibody proliferation rate
ω	Virus replication rate.
θ_1	Immunosuppressive therapy-induced CTL proliferation inhibition rate.
θ_2	Infection-induced CTL proliferation inhibition rate.
Π	Production rate of susceptible cells.

Data sources for parameterization were clearly documented and referenced.

2.3 Model Assumptions

All important assumptions for the formulation of the model were clearly specified.

2.4 Model Simulations

Leveraging our newly developed mathematical model, we conducted simulations to understand how immunosuppressive therapy impacts EVD infection dynamics. These simulations explored the interaction between viral load and immune (CTL and antibody) response during infection. Besides, we used simulations to explore how immunosuppression impacts viral replication and CTL and antibody responses. By analyzing the model's behavior under these different scenarios, we gained valuable insights into the unique dynamics of EVD infection in this specific patient population of immunocompromised individuals.

2.5 Software Application

We used OCTAVE software to conduct an comprehensive analysis of our mathematical model. This analysis included two crucial components. Firstly, we performed sensitivity analysis using these tools. This entailed calculating sensitivity indices, which quantify how variations in key model parameters influence the model's predictions. This allowed us to identify the parameters with the most significant influence on the model's behavior. Secondly, we used the software to simulate the model's response under various conditions. This simulation method offered valuable insights into the potential dynamics of EVD within an immunocompromised patient.

2.6 Model Validation

Ethical considerations prevented us from directly validating our model using data from Ebola patients undergoing immunosuppressive therapy. To overcome this hurdle, we used a technique called sensitivity analysis. This analysis explores how the model's predictions change when we adjust key parameters within realistic ranges. By doing this, we can identify the parameters that have the most significant impact on the model's behavior. We used a specific method called the normalized forward index for this analysis. It is important to note that before conducting the sensitivity analysis, we calculated the basic reproduction number (R_0) using the next generation matrix method.

3. RESULTS AND DISCUSSION

This study used a novel mathematical model to explore how immunosuppressive therapy influences EVD progression within a patient. The model specifically examined the interaction between viral replication, the immune response (CTL and antibody responses) and the effect of this therapy on disease progression.

3.1 Model Development

This section investigates the essential components of our model. We will begin by defining how different populations within the host change over time, a concept known as population dynamics. A visual representation, called a model flow diagram, will then illustrate the interactions between these populations. Finally, to accurately capture the model's behavior, we will translate these interactions into mathematical equations. Key assumptions, variables and parameters will be crucial for this translation.

3.1.1 Model Assumptions

The model was formulated based on the following assumptions

1. **Cell production**

i). Both susceptible cells and viruses are continuously produced at constant rates [2, 3, 26 31, 32].

ii). Both CTLs and antibodies proliferate at constant rates.

2. **Infection**

i). All susceptible cells (macrophages, dendritic and endothelial cells) are equally vulnerable to infection and the infection occurs at a constant rate [2, 3, 31, 32].

3. **Natural cell death**

i). Susceptible cells die naturally at a constant rate [3, 31, 32].

ii). Infected cells, viruses and CTLs die naturally at constant rates [31, 32].

iii). Susceptible and infected cells have equal natural death rates [31, 32].

4. **Immune Response**

i). CTLs eliminate infected cells at a constant rate [31, 32].

ii). Antibodies clear the viruses at a constant rate [23, 32].

iii). Viral infection suppresses CTL proliferation at a constant rate.

iv). Immunosuppressive therapy inhibits CTL and antibody proliferations at constant rates.

5. **Additional Assumptions**

i). The model excludes the possibility of infected cells dying directly from the disease.

ii). The host begins to experience ebolavirus infection in the course of immunosuppressive therapy.

iii). Immunosuppressive therapy inhibits both CTL and antibody proliferation.

3.1.2 Description of Interactions

The model incorporates the complex dynamics between the host's immune response under immunosuppression and EVD. Susceptible cells (macrophages, dendritic cells, and endothelial cells), represented by *S*, are continuously produced at a rate of Π and infected by the viruses at a rate of η. However, both susceptible cells and viruses (*V*), undergo natural death at rates of γ_A and γ_B respectively.

Ebolavirus replication occurs in infected cells (*I*), with new viruses produced at a rate of ω. These infected cells die naturally at a rate of γ_A. The host's cellular immunity is represented by CTLs (*T*) and antibodies (*B*). These CTLs and antibodies show baseline proliferation rates of μ_C and μ_D respectively. However, immunosuppressive therapy and infection of antigen-presenting cells (APCs) themselves function as immunosuppressive forces, reducing CTL and antibody proliferation at rates of θ_2 and θ_1 respectively.

Strengthened and functional CTLs and antibodies are crucial for eliminating infected cells and clearing the viruses respectively. This elimination and clearance processes happen at rates of μ_A and μ_B, proportional to the CTL and antibody populations respectively. Additionally, CTLs die naturally at a rate of γ_C and the antibodies die naturally at a rate of γ_D.

3.1.3 Model Flow Diagram

Drawing on the established understanding of EVD dynamics, Figure 1 presents a flow diagram that summarizes the virus's behavior within an immunosuppressed host. This diagram integrates the model's core assumptions, variable definitions and parameter values.

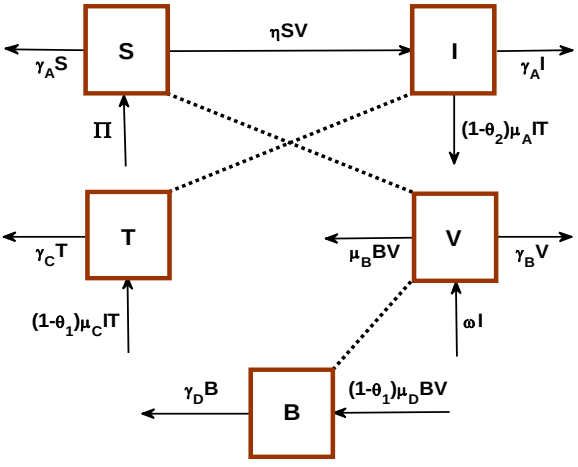

FIGURE 1. Model flow diagram demonstrating the interactions between various populations within an Ebolavirus-infected host undergoing immunosuppressive therapy. Rectangles represent

distinct populations, like uninfected cells or virus particles. Solid arrows indicate the rate of change for each population. Dotted lines, on the other hand, represent interactions that do not directly affect population size, such as virus-host cell contact. The direction of the arrows alongside the rectangles signifies changes in population size: an arrow pointing towards a rectangle indicates an increase, while an arrow pointing away signifies a decrease.

3.1.4 Equations of the Model

Using the model's assumptions, complete interaction descriptions and the model flow diagram provided in Figure 1, we constructed a system of five non-linear ordinary differential equations (ODEs). These equations mathematically capture the dynamic variations in various populations within the host throughout the progression of the Ebola virus infection under immunosuppression.

$$\begin{cases} \dfrac{dS}{dt} = \Pi - \eta SV - \gamma_A S \quad \ldots\ldots(1.1) \\ \dfrac{dI}{dt} = \eta SV - (1-\theta_2)\mu_A IT - \gamma_A I \quad \ldots\ldots(1.2) \\ \dfrac{dV}{dt} = \omega I - \mu_B BV - \gamma_B V \quad \ldots\ldots(1.3) \\ \dfrac{dT}{dt} = (1-\theta_1)\mu_C IT - \gamma_C T \quad \ldots\ldots(1.4) \\ \dfrac{dB}{dt} = (1-\theta_1)\mu_D BV - \gamma_D B \quad \ldots\ldots(1.5) \end{cases}$$

with initial conditions: $S(0) > 0$, $I(0) \geq 0$, $V(0) \geq 0$, $T(0) \geq 0$ and $B(0) \geq 0$.

The ODE model we formulated captures the dynamic interaction between various populations involved in the Ebolavirus infection within an immunosuppressed host. Each equation represents the rate of change for a specific population over time: Equation 1.1 describes the susceptible cell population (S). It considers cell production, infection by the virus and natural cell death. Equation 1.2 focuses on the infected cell population (I). It incorporates the production of infected cells through susceptible cell infection, their natural death and the clearance mediated by the weakened CTL response. Equation 1.3 represents the viral population (V) dynamics. It considers viral production, elimination by antibodies and natural decay. Equation 1.4 models the dynamics of the weakened immune response (T), accounting for its natural decline. Finally, Equation 1.5 describes the antibody population (B) dynamics, considering their production and natural death.

This system of five non-linear ODEs allows us to investigate the complex interactions between these elements during EVD infection in individuals receiving immunosuppressive therapy.

3.2 Qualitative Properties of the Model

The model's qualitative properties play a crucial role in ensuring its validity as a representation of an infectious disease [42]. Mathematically, the solutions generated by the model must be positive, reflecting the real-world existence of cell populations [38]. Additionally, these solutions need to be bounded, allowing the finite number of cells within the human body. Biologically, these mathematical properties translate to realistic scenarios. For example, the model should not predict negative viral loads, which are physically impossible. Also, positively bounded solutions imply that the viral population, after an initial increase, stabilizes below a detectable threshold, preventing the beginning of severe illness [26]. We achieved this validation through lemmas that mathematically demonstrate the positivity and boundedness of our Ebola model.

3.2.1 Positivity of Solutions

Using Theorem 1, we demonstrate that all solutions to the ODE system are always positive.

Theorem 1. If the initial set of variables of the model system $(1.1)-(1.5)$ is $S(0)>0$, $I(0)\geq 0$, $V(0)\geq 0$, $T(0)\geq 0$ and $B(0)\geq 0$, then the solution set $\{S(t),I(t),V(t),T(t),B(t)\}$ will remain positive in $R_+^5 \quad \forall t\geq 0$.

Proof: Positivity. We must prove that the solutions for the state variables $S(t)$, $I(t)$, $V(t)$, $T(t)$ and $B(t)$ will be positive in R_+^5 for all $t\geq 0$. Therefore, we can place lower bounds on each of the equations given in the model. Thus, we have

$$\left.\begin{aligned}
\frac{dS}{dt} &\geq -\eta SV-\gamma_A S\\
\frac{dI}{dt} &\geq -(1-\theta_2)\mu_A IT-\gamma_A I\\
\frac{dV}{dt} &\geq -\mu_B BV-\gamma_B V\\
\frac{dT}{dt} &\geq -\gamma_C T\\
\frac{dB}{dt} &\geq -\gamma_D B
\end{aligned}\right\}. \qquad (2)$$

Solving the set of inequalities (2) with standard methods for differential equations produces

$$S(t) \geq S_0 \exp\left(-\gamma_A t - \eta \int_0^t V(s)ds\right) > 0, \quad I(t) \geq I_0 \exp\left(-\gamma_A t - (1-\theta_1)\mu_A \int_0^t T(s)ds\right) > 0,$$

$$V(t) \geq V_0 \exp\left(-\gamma_B t - \mu_B \int_0^t B(s)ds\right) > 0, \quad T(t) \geq T_0 \exp(-\gamma_C t) > 0 \quad \text{and} \quad B(t) \geq B_0 \exp(-\gamma_D t) > 0.$$

Thus, the variables $S(t)$, $I(t)$, $V(t)$, $T(t)$ and $B(t)$ within the model are always positive for a given context (Ω). This mathematical property, established by Lemma 1, ensures that the model's solutions remain positive in R_+^5 for all time (t) within this context. In simpler terms, the model reflects real-world scenarios where these populations cannot have negative values.

3.2.2 Invariant Region of the Model Solution

This section employs Theorem 2 to identify a region where the solutions of our model remain uniformly bounded. In simpler terms, we will show that all solutions within this specific region will not grow infinitely large over time.

Theorem 2. If the model system $(1.1)-(1.5)$ has initial conditions $S(0) > 0$, $I(0) \geq 0$, $V(0) \geq 0$, $T(0) \geq 0$ and $B(0) \geq 0$, then its solution enters a uniformly bounded region $\Omega \subset R_+^5$ $\forall t \geq 0$, where $\Omega = \Gamma_N \cup \Gamma_V \cup \Gamma_T \cup \Gamma_B \in R_+^2 \times R_+^1 \times R_+^1 \times R_+^1$.

Proof: Boundedness. We must prove that the solutions for the model variables $S(t)$, $I(t)$, $V(t)$, $T(t)$ and $B(t)$ will be bounded for all $t \geq 0$. We achieve this using a piecewise approach as the model incorporates heterogeneous populations

(i). Target Cell Population

We prove that all solutions for the target cell population remain positive over time (positively invariant) within a specific region. Let us represent this region as $\Gamma_N \in R_+^2 (N = S + I)$, defined by the initial condition N_0, evaluated at both S_0 and I_0. Then the total population of the target cells is given by

$$N(t) = S(t) + I(t), \forall t \geq 0.$$

We deduce that

$$\frac{dN(t)}{dt} = \frac{dS(t)}{dt} + \frac{dI(t)}{dt}. \quad (3)$$

Then substituting Equations 1.1 and 1.2 into Equation (3) produces

$$\frac{dN}{dt} = \Pi - (1-\theta_2)\mu_A IT - \gamma_A N. \quad (4)$$

Placing an upper bound on (4) produces

$$\frac{dN}{dt} \le \Pi - \gamma_A N. \quad (5)$$

Solving the inequality (5) with basic differential equation methods produces

$$N(t) \le \frac{\Pi}{\gamma_A} + \left(N_0 - \frac{\Pi}{\gamma_A} \right) \exp(-\gamma_A t). \quad (6)$$

Analysis of (6) reveals the dynamic behavior of the target cell population. When the inequality $N_0 > \Pi/\gamma_A$ holds true, the target cell population asymptotically decreases to Π/γ_A. Conversely, the population increases asymptotically to Π/γ_A when the condition $N_0 < \Pi/\gamma_A$ holds. This implies $N(t) \le \max\{N_0, N^*\}$ for all $t \ge 0$ and whatever value of N_0, wherein $N^* = \Pi/\gamma_A$. This further implies that all solutions for the target cell population enter the region Γ_N, defined by

$$\Gamma_N = \left\{ (S, I) \in R_+^2 : N(t) \le N^* \right\}. \quad (7)$$

Hence, all solutions for the target cell population are positively invariant in the region $\Gamma_N \in R_+^2$. From $N(t) \le N^*$, we deduce that $S(t) \le N^*$ and $I(t) \le N^*$.

(ii). Ebola Virus Population

We demonstrate that all solutions for the Ebolavirus population always remain positive over time (positively invariant) within a defined region. Let us represent this region as $\Gamma_V \in R_+^1$, defined by the initial condition V_0. Then we have:

Placing an upper bound on Equation 1.3 produces

$$\frac{dV}{dt} \le \omega I - \gamma_B V$$

Then, with $I(t) \le N^*$, we deduce that

$$\frac{dV}{dt} \le \omega N^* - \gamma_B V \tag{8}$$

Solving the inequality (8) using basic differential equation methods produces

$$V(t) \le \frac{\omega N^*}{\gamma_B} + \left(V_0 - \frac{\omega N^*}{\gamma_B} \right) \exp(-\gamma_B t) \tag{9}$$

Our analysis of (9) reveals the dynamic behavior of ebolavirus population. When the condition $V_0 > \omega N^* / \gamma_B$ holds true, the ebolavirus population asymptotically decreases to $\omega N^* / \gamma_B$. Conversely, when the condition $V_0 < \omega N^* / \gamma_B$ applies, it increases asymptotically to $\omega N^* / \gamma_B$. This implies that $V(t) \le \max\{V_0, V^*\}$ for all $t \ge 0$ and any value of V_0, where $V_0 = \omega N^* / \gamma_B$. This further implies that all solutions for ebolavirus population enter the region Γ_V, defined by

$$\Gamma_V = \left\{ V \in R_+^1 : V(t) \le V^* \right\}. \tag{10}$$

Thus, all solutions for ebolavirus population are positively invariant in the region $\Gamma_V \in R_+^1$.

(iii). CTL Population

We prove that all solutions for the CTL population always remain positive over time (positively invariant) within a defined region. Let us represent this region as $\Gamma_T \in R_+^1$, defined by the initial condition T_0. Then we have:

Substituting $I(t) \le N^*$ into Equation 1.4 produces.

$$\frac{dT}{dt} \le (1-\theta_1)\mu_C N^* T - \gamma_C T ,$$

which can be expressed as

$$\frac{dT}{dt} \le ((1-\theta_1)\mu_C N^* - \gamma_C) T . \tag{11}$$

Solving inequality (11) with basic differential equation methods produces

$$T(t) \le T_0 \exp[((1-\theta_1)\mu_C N^* - \gamma_C)t] . \tag{12}$$

Analysis of (12) reveals that $T(t)$ is bounded above only if $(1-\theta_1)\mu_C N^* - \gamma_C \le 0$ for all $t \ge 0$. Therefore, $T(t) \le T_0$. This implies that all solutions for the CTL population are positively invariant within the region $\Gamma_T \in R_+^1$, defined by

$$\Gamma_T = \{T \in R_+^1 : T(t) \le T_0\}. \qquad (13)$$

(iv). Antibody Population

We demonstrate that all solutions for the antibody population always remain positive over time (positively invariant) within a defined region. Let us represent this region as $\Gamma_B \in R_+^1$, defined by the initial condition B_0. Then we have:

Substituting $V(t) \le V^*$ into Equation 1.5 produces

$$\frac{dB}{dt} \le (1-\theta_1)\mu_D B V^* - \gamma_D B,$$

which can be expressed as

$$\frac{dB}{dt} \le ((1-\theta_1)\mu_D V^* - \gamma_D)B \qquad (14)$$

Solving inequality (14) with basic differential equation methods produces

$$B(t) \le B_0 \exp[((1-\theta_1)\mu_D V^* - \gamma_D)t]. \qquad (15)$$

Analysis of (15) shows that $B(t)$ is bounded above only if $(1-\theta_1)\mu_D V^* - \gamma_D \le 0$ hold true for all $t \ge 0$. Hence, $B(t) \le B_0$. This implies that all solutions for the antibody population are positively invariant the region Γ_B, defined by

$$\Gamma_B = \{B \in R_+^1 : B(t) \le B_0\} \qquad (16)$$

With the analytical results (7), (10), (13) and (16), we can establish that all solutions of the entire system $(1.1)-(1.5)$ are positively invariant in the region $\Omega \in R_+^5$. This is because $\Omega \in R_+^5$ implies that $\Omega = \Gamma_N \times \Gamma_V \times \Gamma_T \times \Gamma_B \in R_+^2 \times R_+^1 \times R_+^1 \times R_+^1$, where

$$\Gamma_N = \left\{(S,I) \in R_+^2 : N(t) \le N^*\right\},$$

$$\Gamma_V = \left\{V(t) \in R_+^1 : V(t) \le V^*\right\},$$

$$\Gamma_T = \{T(t) \in R_+^1 : T(t) \le T_0\}.$$

and $$\Gamma_B = \{B(t) \in R_+^1 : B(t) \le B_0\}.$$

Hence, the model $(1.1)-(1.5)$ is mathematically and biologically realistic [16].

3.3 Existence of Model Equilibrium States

An infectious disease is endemic whenever it persists in a population and the population is free if the disease does not persist in it [13, 20]. The equilibrium state $(S^*, I^*, V^*, T^*, B^*)$ of the model is obtained by setting the model equations $(1.1)-(1.5)$ equal to zero and solving for the state variables. Therefore, we have the following system.

$$\begin{cases} \Pi - \eta SV - \gamma_A S = 0 \\ \eta SV - (1-\theta_2)\mu_A IT - \gamma_A I = 0 \\ \omega I - \mu_B BV - \gamma_B V = 0 \\ (1-\theta_1)\mu_C IT - \gamma_C T = 0 \\ (1-\theta_1)\mu_D BV - \gamma_D B. = 0 \end{cases} \tag{17}$$

Using the system (17), we can obtain the model equilibria as follows.

3.3.1 Disease-Free Equilibrium Point

We derive the disease-free equilibrium point (E_0) when $I^* = V^* = T^* = B^* = 0$. Therefore, the equilibrium point is $E_0 = (\Pi/\gamma_A, 0, 0, 0, 0)$.

3.3.2 Endemic Equilibrium Point

We derive the endemic equilibrium point (E^*) when $I^* \neq V^* \neq T^* \neq B^* \neq 0$. Therefore, the equilibrium point is $E^* = (S^*, I^*, V^*, T^*, B^*)$, where $S^* = \dfrac{(1-\theta_1)\Pi\mu_D}{Q}$, $I^* = \dfrac{\gamma_C}{(1-\theta_1)\mu_C}$, $V^* = \dfrac{\gamma_D}{(1-\theta_1)\mu_D}$, $T^* = \dfrac{\gamma_C(1-\theta_1)(\Pi Q - (1-\theta_1)\gamma_A\gamma_D) - \gamma_A\gamma_D Q}{\gamma_C(1-\theta_2)\mu_A Q}$, $B^* = \dfrac{\omega\gamma_C - \gamma_B\gamma_D}{\gamma_D\mu_B}$ and $Q = \eta\gamma_D + (1-\theta_1)\gamma_A\gamma_D$.

3.4 Basic Reproduction Number

Infectious diseases spread through transmission between individuals. A fundamental metric in understanding this spread is the basic reproduction number (R_0), defined as the average number of secondary cases caused by one infectious individual introduced in a completely susceptible population [18, 22]. This number addresses and quantifies the ability of an infectious disease to invade a purely susceptible population [18, 22]. The epidemic persists when $R_0 > 1$ and dies out when the $R_0 < 1$ [16, 19. 25, 27]. We compute R_0 using the next generation method as proposed by Van den Driessche and Watmough [27], Diekmann and Heesterbeek [24]. This method has been implemented in various studies, including those by Osman et al. [37], Mpeshe et al. [30], Osman et al. [36] and Ismail [32].

Then, considering our EVD dynamics model, we initially define the system for infections in compartments as

$$\frac{dY_i}{dt} = K_i - L_i,$$

where Y_i defines the set of infected class, K_i defines the rate of new infections in compartment i, and $L_i = L_i^- - L_i^+$ defines the total transfer rate, L_i^- describes the transfer rate of individuals out of compartment i and L_i^+ is the transfer rate of individuals into compartment i through interactions. Then using Equations (1.2) and (1.3), we have .

$$\begin{bmatrix} \frac{dI}{dt} \\ \frac{dV}{dt} \end{bmatrix} = K_i - L_i = \begin{bmatrix} \eta SV \\ \omega I \end{bmatrix} - \begin{bmatrix} (1-\theta_2)\mu_A IT + \gamma_A I \\ \mu_B BV + \gamma_B V \end{bmatrix}. \qquad (18)$$

The corresponding Jacobian matrices K and L are the matrices of the derivatives of K_i and L_i with respect to $I(t)$ and $V(t)$ at the disease-free equilibrium point, E_0. They are given by

$$K = \left[\frac{\partial K_i(E_0)}{\partial X_j}\right] = \begin{bmatrix} 0 & \frac{\eta\Pi}{\gamma_A} \\ \omega & 0 \end{bmatrix} \qquad (19)$$

$$L = \left[\frac{\partial L_i(E_0)}{\partial X_j}\right] = \begin{bmatrix} \gamma_A & 0 \\ 0 & \gamma_B \end{bmatrix}.$$

We deduce that

$$L^{-1}=\begin{bmatrix}\frac{1}{\gamma_A} & 0\\ 0 & \frac{1}{\gamma_B}\end{bmatrix}. \tag{20}$$

Let G be the next generation matrix defined by $G=KL^{-1}$, where

$$G=KL^{-1}=\left[\frac{\partial K_i(E_0)}{\partial X_j}\right]\left[\frac{\partial L_i(E_0)}{\partial X_j}\right]^{-1}. \tag{21}$$

Then substituting (19) and (20) into (21) produces

$$G=\begin{bmatrix}0 & \frac{\eta\Pi}{\gamma_A}\\ \omega & 0\end{bmatrix}\begin{bmatrix}\frac{1}{\gamma_A} & 0\\ 0 & \frac{1}{\gamma_B}\end{bmatrix}=\begin{bmatrix}0 & \frac{\eta\Pi}{\gamma_A\gamma_B}\\ \frac{\omega}{\gamma_A} & 0\end{bmatrix}.$$

The eigenvalues of matrix G are given by

$$\left|\lambda I-G\right|=\left|\lambda I-KL^{-1}\right|=0,$$

where

$$\lambda I-G=\begin{bmatrix}\lambda & 0\\ 0 & \lambda\end{bmatrix}-\begin{bmatrix}0 & \frac{\eta\Pi}{\gamma_A\gamma_B}\\ \frac{\omega}{\gamma_A} & 0\end{bmatrix}=\begin{bmatrix}\lambda & -\frac{\eta\Pi}{\gamma_A\gamma_B}\\ -\frac{\omega}{\gamma_A} & \lambda\end{bmatrix}.$$

Thus, we have

$$\left|\lambda I-KL^{-1}\right|=0\Rightarrow\begin{vmatrix}\lambda & -\frac{\eta\Pi}{\gamma_A\gamma_B}\\ -\frac{\omega}{\gamma_A} & \lambda\end{vmatrix}=0. \tag{22}$$

From (22), the eigenvalues of G are

$$\lambda_1=\sqrt{\frac{\omega\eta\Pi}{(\gamma_A)^2\gamma_B}}\quad\text{and}\quad\lambda_2=-\sqrt{\frac{\omega\eta\Pi}{(\gamma_A)^2\gamma_B}}.$$

The basic reproduction number (R_0) is the spectral radius of the next generation matrix G, which is the dominant eigenvalue [27]. That is,

$$R_0=\rho(G)=\max(\lambda_1,\lambda_2)=\sqrt{\frac{\omega\eta\Pi}{(\gamma_A)^2\gamma_B}}.$$

Thus, the basic reproduction number, R_0 is

$$R_0 = \sqrt{\frac{\omega\eta\Pi}{(\gamma_A)^2\gamma_B}}\,. \qquad (23)$$

The result shown in (23) reveals that R_0 for this model system is primarily driven by factors related to viral transmission and natural lifespans [43]. These factors comprise the rate of virus production by infected cells, the rate of susceptible cell infection, and the natural death rates of susceptible cells, infected cells, and the virus. Obviously, the model suggests that the immune response, characterized by CTLs, does not influence R_0. This is because R_0 focuses exclusively on the initial stages of infection before a significant immune response has time to develop [29].

From epidemiological standpoint, the model allows us to predict the fate of the infection within the host. If specific parameter values meet a threshold (represented by $R_0 < 1$), the host's immune system effectively controls the infection, leading to its eventual disappearance. On the other hand, if these parameters fall below another threshold (represented by $R_0 > 1$), the infection gains a foothold and persists within the host.

3.5 Sensitivity Analysis

To understand how changes in a model's components affect its predictions, we can employ a powerful technique called sensitivity analysis. This analysis calculates sensitivity indices, which reveal how much each parameter influences key outputs. In this study, we use the normalized forward index [21] to perform a sensitivity analysis on R_0 within our Ebola model that focused on individual hosts.

R_0, typically used in population models, represents the average number of secondary infections caused by one infected person in a susceptible population. However, by pinpointing the cellular factors influencing R_0 within a single host, we can gain valuable insights for controlling Ebola outbreaks at their earliest stages. This analysis aims to identify the parameters within the host model that have the most significant impact on R_0 by calculating their sensitivity indices. This knowledge can then be used to develop targeted strategies to control Ebola transmission during the initial stages of infection.

We performed the sensitivity analysis using parameter values obtained from relevant literature. The specific values used for the analysis include: $\Pi = 1.05$ [38], $\eta = 0.0027$ [38], $\omega = 40.9$ [38], $\gamma_A = 0.02$ [38], $\gamma_B = 1.15$ [39]. The following method was employed to calculate the sensitivity indices.

Definition: The sensitivity index of R_0 with respect to parameter W is defined as

$$\mathrm{X}_W^{R_0} = \frac{W}{R_0} \times \frac{\partial R_0}{\partial W},$$

provided that R_0 is differentiable with respect to W.

Hence, the sensitivity indices of R_0 with respect to parameters γ_A and η are given by

$$\mathrm{X}_{\gamma_A}^{R_0} = \frac{\gamma_A}{R_0} \times \frac{\partial R_0}{\partial \gamma_A} = -3.98445 \text{ and } \mathrm{X}_{\eta}^{R_0} = \frac{\eta}{R_0} \times \frac{\partial R_0}{\partial \eta} = +1.99222.$$

The sensitivity indices of other parameters (γ_A, ω and Π) are obtained similarly, and all indices are enumerated in Table 2.

TABLE 2. Numerical values of sensitivity indices of R_0.

Parameter Symbol	**Sensitivity Index**
γ_A	-3.98445
γ_B	-1.99222
ω	+1.99222
η	+1.99222
Π	+1.99222

Sensitivity indices, as shown in Table 2, provide understandings of how key parameters impact R_0 within our model. Positive indices, like those for parameters connected to production rate of susceptible cells (Π), virus production rate (ω), and infection rate (η), show that R_0 increases as these parameters increase (assuming all others stay constant). This suggests a higher potential for the disease to become more widespread. On the other hand, negative indices correspond to parameters where a higher value leads to a decrease in R_0. This applies to parameters like the natural death rate of susceptible cells (γ_A) and the natural death rate of the virus (γ_B). A higher natural death rate for either susceptible cells or virus particles obstructs the virus's ability to spread, implying a lower disease prevalence.

Sensitivity indices shed light on the most critical factors governing our model's outcome. The analysis reveals that the natural death rate of susceptible cells (γ_A) emerges as the most sensitive parameter. This implies that even minor fluctuations in the natural death rate of susceptible cells can significantly influence the model's predictions. Compared to (γ_A), other

parameters like the natural death rate of the virus (γ_B), virus production rate (ω), infection rate (η) and production rate of new susceptible cells (Π) exert a lesser influence.

3.6 Numerical Simulations

Ebola's complex within-host interactions need computational modeling for comprehensive analysis [40]. Numerical simulations serve as virtual laboratories, mimicking viral replication and the host's immune response in individuals receiving immunosuppressive therapy [6]. In this study, we employed simulations to investigate these dynamics, incorporating parameters listed in Table 3. This in silico approach provides a safe and controlled environment to explore potential treatment strategies, ultimately accelerating the improvement of effective interventions for immunocompromised patients during Ebola outbreaks.

TABLE 3. Parameter values used for simulations of the model.

Parameter Symbol	**Unit**	**Parameter Value**	**Source**
η	*cell* day^{-1}	0.0027	[38]
γ_A	*cell* mil^{-1} day^{1}	0.15	Estimated
γ_B	*virus* $cell^{-1}$ day^{-1}	0.15	Estimated
γ_C	*cell* day^{-1}	0.015	Estimated
γ_D	*cell* day^{-1}	0.02	[23]
μ_A	*cell* day^{-1}	0.01	Estimated
μ_B	*virus* day^{-1}.	0.01	Estimated
μ_C	*cell* day^{1}	0.001	Estimated
μ_D	*cell* day^{1}	0.001	Estimated
ω	*virus* $cell^{-1}$ day^{-1}	4.9	Estimated
θ_1		0.9	Estimated
θ_2		0.3	Estimated
Π	*cells* mil^{-1} day^{1}	125.5	Estimated

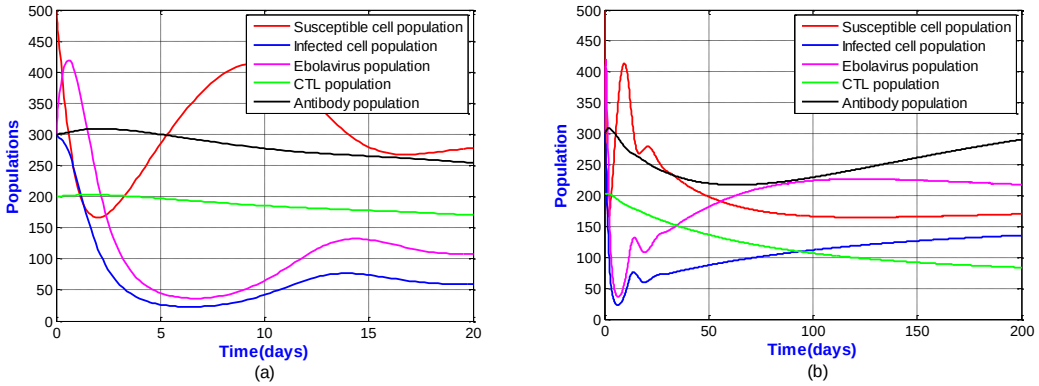

FIGURE 2. Trajectories of the model populations demonstrating EVD dynamics.

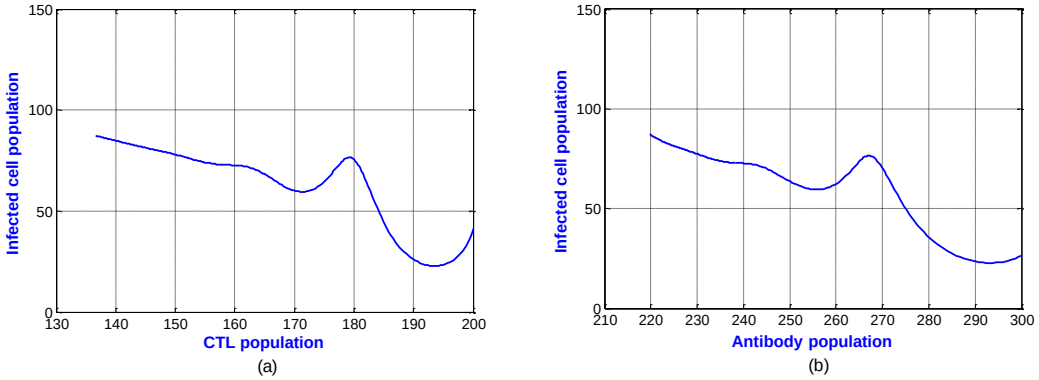

FIGURE 3. The effect of weakened CTL and antibody responses on the infected cell population.

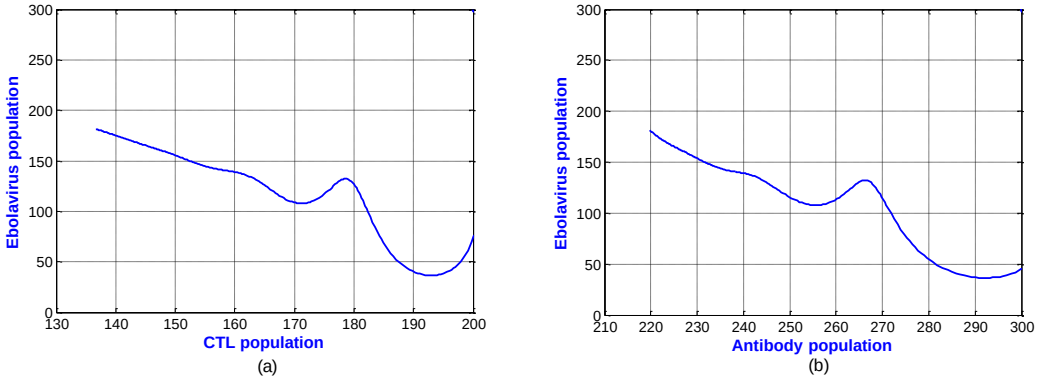

FIGURE 4. The effect of weakened CTL and antibody responses on the virus population.

Figures 2(*a*), (*b*) exhibit how immunosuppressive therapy influences EVD within patients. Immunosuppression weakens the immune response, obstructing the production of CTLs (cell killers) and antibodies (virus neutralizers). This reduces the elimination of infected cells and viral deactivation, respectively. Consequently, infected cell and virus populations rise sharply (Figures 3(*a*), (*b*) and Figures 4(*a*), (*b*)). With more infected cells persisting, virus production increases,

prompting a subsequent rise in antibodies. However, this increase in virus also leads to a decline in susceptible cells, as they become infected.

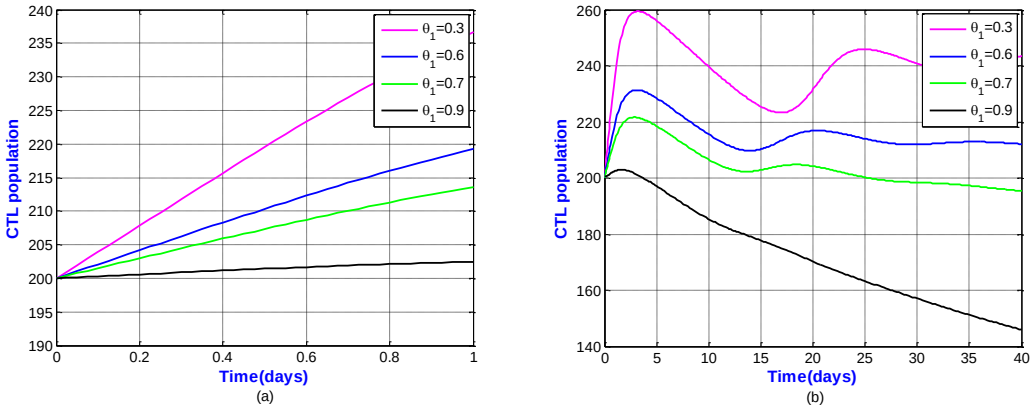

FIGURE 5. The effect of immunosuppressive therapy on the CTL population.

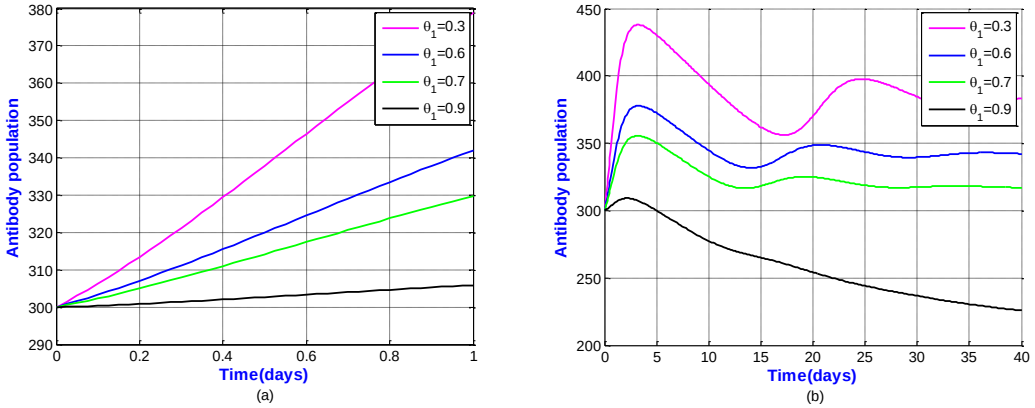

FIGURE 6. The effect of immunosuppressive therapy on the antibody population.

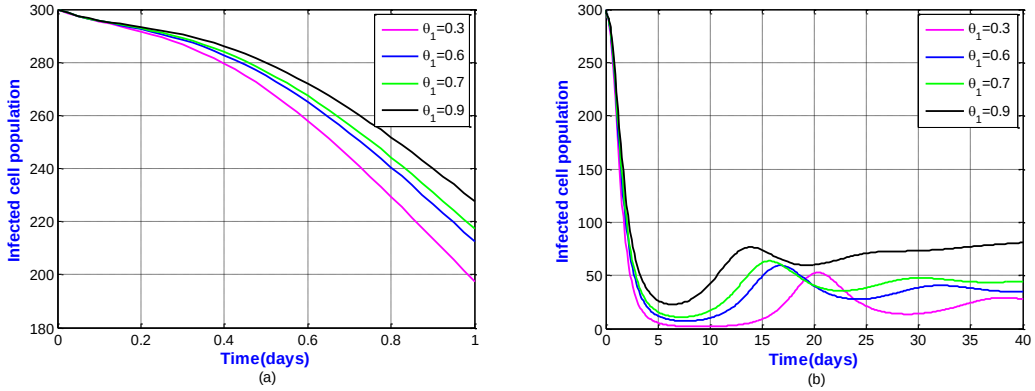

FIGURE 7. The effect of immunosuppressive therapy on the infected cell population

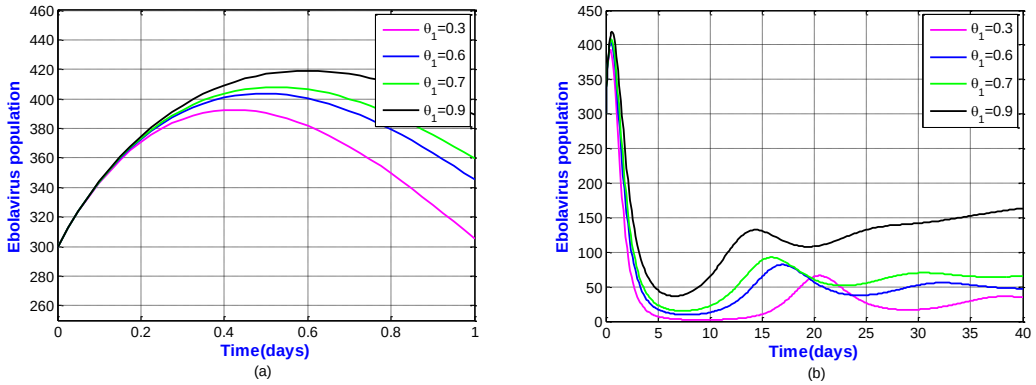

FIGURE 8. The effect of immunosuppressive therapy on the virus population

Figures 5(*a*), (*b*) and Figures 6(*a*), (*b*) exhibit that a higher efficacy of immunosuppressive therapy suppresses the growth of CTLs (cell killers) and antibodies (virus neutralizers), leading to lower populations of each (Figures 5(*a*), (*b*) and Figures 6(*a*), (*b*)). This translates to an increase in infected cells (Figures 7(*a*), (*b*)), which in turn rise virus production (Figures 8(*a*), (*b*)). With fewer antibodies to deactivate viruses, the viral load and infected cell population increase.

4. CONCLUSION

This study employed mathematical modeling to explore how immunosuppressive therapy impacts EVD within a patient. The model incorporated viral replication, immune responses (CTL and antibody) and the effects of varying immunosuppression levels. Simulations revealed a critical finding: increased immunosuppression directly correlated with a rise in viral replication and a weakened immune response.

These findings illuminate the potential risks associated with immunosuppressive therapy during EVD outbreaks. While this therapy remains crucial for some patients with underlying conditions, it can inadvertently exacerbate the severity and duration of the viral infection. This highlights the importance of carefully considering this complex interaction when making treatment decisions for EVD patients requiring immunosuppression.

The in silico approach employed here provides valuable insights for future research. By refining the model with additional biological details and integrating real-world clinical data, researchers can further strengthen these conclusions. Ultimately, this study paves the way for developing improved treatment strategies for EVD patients, particularly those requiring immunosuppressive therapy, by enabling a more balanced approach that considers both the

benefits of the therapy and the potential risks of compromising the immune system's ability to fight the virus.

ACKNOWLEDGEMENTS

I express my sincere thanks to the Benjamin Mkapa Hospital administration for their unique support. Access to their esteemed epidemiology team and transplant nephrologists was necessary for my Ebola disease research.

CONFLICTS OF INTEREST

The author declares there is no conflict of interests.

REFERENCES

[1] A.K. Abbas, A.H. Lichtman, Basic immunology: Functions and disorders of the immune system, 6th ed. Elsevier, 2020.

[2] A. Perelson, P. Nelson, Mathematical analysis of hiv-1 dynamics in vivo, SIAM Rev. 41 (2001), 3-43.

[3] A. Perelson, Modelling viral and immune system dynamics, Nat. Rev. Immunol. 2 (2002), 28–36.

[4] B. Gu, J. Wang, H. Zhu, A mathematical model for Ebola virus disease with immune response and immunosuppression, Chaos Solitons Fractals, 13 (2020).

[5] C.H. Meyer, R.A. Begum, C.M. Sorrell, A mathematical model to assess the efficacy of antiviral therapies for Ebola virus disease in immunocompromised patients, Bull. Math. Biol. 83 (2021), 1-22.

[6] C.J. Haas, et al., Immunomodulatory effects of therapeutic interventions for Ebola virus disease, Clin. Microbiol. Rev. 31 (2018), e00062-18.

[7] C.R. Bauer, T. Britton, M.L. Mbow, et al. The impact of vaccination coverage on the transmission dynamics of Ebola virus disease, Epidemics, 28 (2019), 100342.

[8] D. Gao, J. Lou, J. He, et al. Modeling the immune response to Ebola virus vaccination, Viruses, 13 (2021), 127.

[9] D. Gatherer, M. Doherty, Evolving strategies for the development of vaccines against Ebola virus, Phil. Trans. R. Soc. B: Biol. Sci. 369 (2014), 20130456.

[10] D.O. Oganga, Mathematical analysis of a within host Ebola disease model, Appl. Math. Sci. 14 (2020), 433-448.

[11] D.S. Chertow, L. Shekhtman, Y. Lurie, et al. Modeling challenges of Ebola virus–host dynamics during infection and treatment, J. Theor. Biol. 500 (2020), 242-253.

[12] G. Chowell, H. Nishiura, C. Viboud, Transmission dynamics of Ebola virus disease during outbreaks, Lancet Infect. Dis. 16 (2016), e144-e157.

[13] G.G. Mwanga, et al., Mathematical modeling and optimal control of malaria, PhD Thesis, Acta Lappeenranta University, 2014.

[14] G. Warren, W.A. Rutala, Ebola virus disease, N. Engl. J. Med. 381 (2019), 657-666.

[15] H. Feldmann, T.W. Geisbert, P.B. Jahrling, Ebola virus disease, in: G. P. Wormsley & G. L. Brook (Eds.), Infectious Diseases: A Treatise on Emerging and Established Infections, pp. 1-22. Elsevier, 2022.

[16] H.W. Hethcote, The mathematics of infectious diseases, SIAM Rev. 42 (2000), 599–653.

[17] H.Y. Haddock, T.K. Warren, W.A. Rutala, Filoviridae: hemorrhagic fever viruses, in: Mandell, Douglas and Bennett's Principles and Practice of Infectious Diseases, vol. 2, pp. 1613-1633. Elsevier, 2020.

[18] I.M. Foppa, The basic reproductive number of tick–borne encephalitis virus, J. Math. Biol. 51 (2005), 616-628.

[19] J. Wang, C. Modnak, Modeling cholera dynamics with controls, Canad. Appl. Math. Quart. 19 (2011), 255–273.

[20] M.A. Selemani, L.S. Luboobi, Y. Nkansah-Gyekye, On stability of the in-human host and in-mosquito dynamics of malaria parasite, Asian J. Math. Appl. 2016 (2016), 23.

[21] M.C. Marino, C.D. Baxter, J. Naveau, et al. Methodology for modeling and analyzing complex ecological systems with uncertain components, Ecol. Model. 211 (2008), 164-182.

[22] N. Hartemink, S. Randolph, S. Davis, et al. The basic reproduction number for complex disease systems: Defining r0 for tick-borne infections, Amer. Naturalist, 171 (2008), 743–754.

[23] N.O. Lasisi, N.I. Akinwande, R.O. Olayiwola, et al. Mathematical model for Ebola virus infection in human with effectiveness of drug usage, J. Appl. Sci. Environ. Manage. 22 (2018), 1089-1095.

[24] O. Diekmann, J.A.P. Heesterbeek, Mathematical epidemiology of infectious diseases: Model building, analysis and interpretation, John Wiley & Sons, 2000.

[25] O. Diekmann, J.A.P. Heesterbeek, J.A.J. Metz, On the definition and the computation of the basic reproductive ratio R_0 in models for infectious diseases in heterogeneous populations, J. Math. Biol. 28 (1990), 365-382.

[26] P.A. Roemer, Stochastic modeling of the persistence of HIV: Early population dynamics, Trident Scholar Project Report, no. 420, United States Naval Academy, US, 2013.

[27] P. Van Den Driessche, J. Watmough, Reproduction numbers and sub-threshold endemic equilibria for compartmental models of disease transmission, Math. Biosci. 180 (2002), 29-48.

[28] Q. Li, Y. Liu, M. Jin, Mathematical modeling for evaluating the effectiveness of vaccination strategies against Ebola virus disease, BMC Infect. Dis. 23 (2023), 1-10.

[29] R.M. Anderson, R.M. May, Infectious diseases of humans: Dynamics and control, Oxford University Press, 1991.

[30] S.C. Mpeshe, L.S. Luboobi, Y. Nkansah-Gyekye, Modeling the impact of climate change on the dynamics of rift valley fever, Comput. Math. Methods Med. 201 (2014), 1-12.

[31] S. Ismail, A.P. Mtunya, A mathematical analysis of an in-vivo Ebola virus transmission dynamics model, Tanzania J. Sci. 47 (2021), 1464–1477.

[32] S. Ismail, Mathematical analysis of in-host Ebola virus infection dynamics model with sensitivity analysis, Ethiopian J. Sci. Technol. 16 (2023), 181-207.

[33] S.J. Raffel, D.H. Olson, D.W. Kaufman, et al. The challenge of Ebola virus disease in solid organ transplant recipients: A case report and review of the literature, Transplant. Direct, 8 (2020), e341.

[34] S.M. Moore, R.M. Anderson, Epidemic dynamics and control of dracunculiasis, Nature, 377 (1996), 131-133.

[35] S. Mulangu et al., A randomized, controlled trial of Ebola virus disease therapeutics, N. Engl. J. Med. 381 (2019), 2293-2303.

[36] S. Osman, D. Otoo, C. Sebil, Bifurcation, sensitivity and optimal control analysis of modeling anthrax-listeriosis co-dynamics, Comm. Math. Biol. Neurosci. 2020 (2020), 98.

[37] S. Osman, O.D. Makinde, H.A. Togbenon, et al. Mathematical modeling of dynamics of campylobacteriosis using nonstandard finite difference approach with optimal control, Comput. Math. Methods Med. 2020 (2020), 1-12.

[38] T. Wester, Analysis and simulation of a mathematical model of Ebola virus dynamics in vivo, SIURO, 8 (2015), 236–256.

[39] V.K. Nguyen, S.C. Binder, A. Boianelli, et al. Ebola virus infection modeling and identifiability problems, Front. Microbiol. 6 (2015), 1–11.

[40] W.J. Wiersinga, M.D. de Jong, M.P. Koopmans, Ebola virus disease, The Lancet, 384 (2014), 1656-1666.

[41] World Health Organization (WHO), Ebola virus disease, 2016.
Retrieved from http://apps.who.int/iris/bitstream/10665/205945/1/ebolasitrep_5may2016_eng.pdf?ua=1

[42] X. Ji, J. Sun, H. Miao, A multi-strain SEIR model with saturated incidence for infectious diseases, Chaos Solitons Fractals, 138 (2020), 110302.

[43] Y. Liu, Y. Zhang, F. He, A mathematical model for Ebola virus disease with saturated incidence and CTL immune response, BMC Infect. Dis. 16 (2016), 740.

[44] Z. Wang, J. Xu, M. Jin, CRISPR-Cas systems for the treatment of Ebola virus disease: a mathematical modeling approach, Front. Public Health, 10 (2022), 820954.